PHYSICAL REVIEW E **75**, 050404(R) (2007)

Statistical mechanics of the glass transition as revealed by a Voronoi tesselation

H. G. E. Hentschel,[1] Valery Ilyin,[2] Nataliya Makedonska,[2] Itamar Procaccia,[2] and Nurith Schupper[2]
[1]*Department of Physics, Emory University, Atlanta, Georgia 30322, USA*
[2]*The Department of Chemical Physics, The Weizmann Institute of Science, Rehovot 76100, Israel*
(Received 17 August 2006; published 30 May 2007)

The statistical mechanics of simple glass forming systems in two dimensions is worked out. The glass disorder is encoded via a Voronoi tesselation, and the statistical mechanics is performed directly in this encoding. The theory provides, without free parameters, an explanation of the glass transition phenomenology, including the identification of two different temperatures, T_g and T_c, the first associated with jamming and the second associated with crystallization at very low temperatures.

DOI: 10.1103/PhysRevE.75.050404 PACS number(s): 61.43.Hv, 05.45.Df, 05.70.Fh

INTRODUCTION

The term "glass transition" refers to the enormous slowing down in the dynamics of some liquids when their temperature is lowered. Despite decades of research, a clear explanation of this phenomenon, common to materials as diverse as molecular glasses, metallic glasses, colloids, etc., is still lacking [1]. The difficulty is that the disordered molecular arrangement in a glass appears indistinguishable from that of the corresponding liquid, without any sign of a static correlation length that increases appreciably at the glass transition [2]. In this Rapid Communication, we offer a theory of the glass transition in simple glass forming systems, based on an encoding of the disorder that is able to flush out the pertinent features of the transition. In particular, the disappearance of liquidlike regions and the huge increase of a typical scale are all understood, in agreement with numerical simulations.

The system. We focus again on the well-studied glass former obtained from a two-dimensional binary mixture of disks interacting via a soft $1/r^{12}$ repulsion with a "diameter" ratio of 1.4 [3]. The particles have the same mass m, but half of the particles are "large" with "diameter" $\sigma_2=1.4$ and half of the particles are "small" with "diameter" $\sigma_1=1$. The three pairwise additive interactions are purely repulsive:

$$u_{ab}=\epsilon\left(\frac{\sigma_{ab}}{r}\right)^{12}, \quad a,b=1,2, \tag{1}$$

where $\sigma_{aa}=\sigma_a$ and $\sigma_{ab}=(\sigma_a+\sigma_b)/2$. The cutoff radii of the interaction are set at $4.5\sigma_{ab}$. The units of mass, length, time, and temperature are m, σ_1, $\tau=\sigma_1\sqrt{m/\epsilon}$, and $T=\epsilon/k_B$, respectively, with k_B being Boltzmann's constant. We simulated $N=1024$ particles in a square box (of area L^2) with periodic boundary conditions. Reference [3] found that for temperature $T>0.5$ the system is liquid and for lower temperatures dynamical relaxation slows down. A precise glass transition had not been identified in [3].

The glass transition. To overcome the lack of signatures of the glass transition in the particle positions on the molecular level, we encode the state of the system using the Voronoi tesselation [5], where a polygon associated with any particle contains all points closest to that particle than to any other particle. The edges of such a polygon are the perpendicular bisectors of the vectors joining the central particle. Such an encoding has been used extensively before [3–5], where it was also noted that the geometric Euler constraint implies that average coordination number is 6 at all temperatures, and local coordination numbers other than 6 were referred to as "defects." Our encoding is richer; in our work [6] it was discovered that a significant insight to the glass transition is gained by distinguishing between "liquidlike" defects and "glasslike" defects. We observed [6] that only in the liquid phase there exist small particles enclosed in heptagons (or even octagons), and large particles enclosed in pentagons (or even squares) (cf. Fig. 1, right panel). In the glass phase, we observe only defects of the opposite type, i.e., small particles in pentagons and large particles in heptagons, see Fig. 1. Accordingly we proposed that the concentration of these particular defects is a good indicator of the glass transition. The concentration c_ℓ of these liquidlike defects becomes so small in the glass phase that we cannot distinguish it from zero (cf. Fig. 1, lower panel), unless the glass is put under mechanical strain, cf. Ref. [6]. Associated with this concentration, we can define a typical scale, ξ:

$$\xi \equiv 1/\sqrt{c_\ell}. \tag{2}$$

In parallel with the strong decrease in c_ℓ, we observe a huge increase in the typical scale ξ, in agreement with the tremendous slowing down of the dynamics [7].

In Fig. 2, right panel, we show c_ℓ as a function of the temperature for a protocol of slow cooling. For temperatures larger than 0.8, the concentration follows closely an exponential fit,

$$c_\ell = A\exp-(\Delta U/T), \quad A\approx 0.094, \quad \Delta U\approx 1.90. \tag{3}$$

For temperatures in the range $0.3<T<0.8$, we find an excellent fit to

$$c_\ell = B(T-T_g)^2, \quad B\approx 0.02, \quad T_g=0.16\pm 0.02. \tag{4}$$

The quality of this fit is demonstrated in Fig. 2, left panel. The fit (4) appears to identify a sharp glass transition $T_g=0.16\pm0.02$; note, however, that the fit is made in the range $0.3<T<0.8$ that does not include T_g. In fact, there is no theoretical reason to expect that c_ℓ truly vanishes at T_g, but it becomes so small that we indeed do not see a single liquidlike defect in our finite-box simulations. Similarly, in our finite size box we cannot distinguish between a diverging length scale and a scale much larger than L. Within the range $0.3<T<0.8$, we fit an apparently divergent length

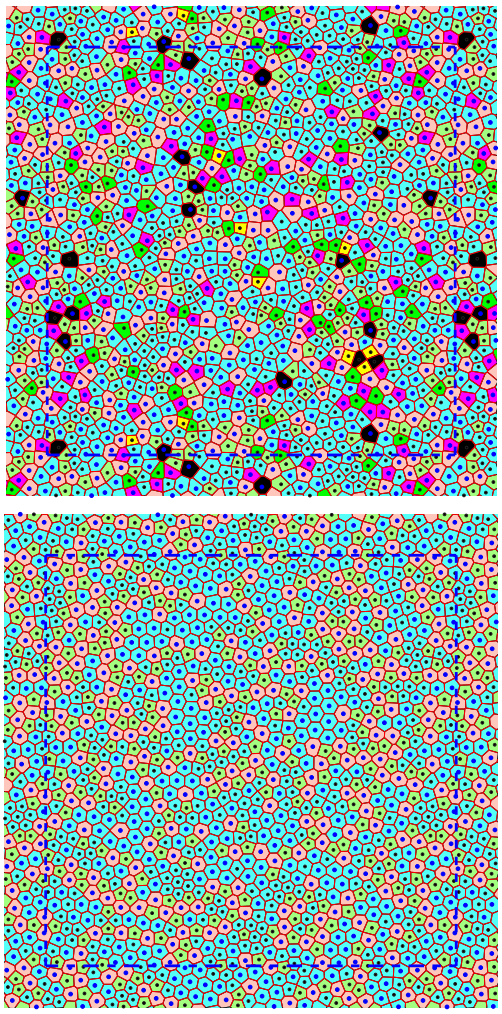

FIG. 1. (Color online). Upper panel: a Voronoi polygon construction at $T=3$, with the seven-color code used in this paper. Small particles in pentagons (heptagons) are light green (dark green) and large particles in pentagons (heptagons) are violet (pink). Hexaons are in blue, octagons in black, and squares in yellow. Lower panel: a typical Voronoi construction in the glass phase at $T=0.1$. Note the total disappearance of liquidlike defects.

$$\xi \sim (T - T_g)^{-\nu}, \quad \nu = 1. \tag{5}$$

In [6], it was shown that the divergence of ξ is in one-to-one correspondence with the divergence of the relaxation time of the viscous fluid as $T \to T_g$.

Statistical Mechanics. Here, we present the statistical mechanics of this system, rationalizing and explaining the features of the transition presented above. The main point to stress is that even in the glass phase, when particles are practically jammed and precluded from large excursions, the Voronoi tesselation is still highly mobile. Minute changes in particle positions can lead, via T1 foamlike processes [8], to transitions between cell types. Therefore if one can convince oneself that the cell types, including the presence of a small or large particle inside them, are proper "species," one can construct statistical mechanics right on the space of these cells. We define the energy of each cell type as the average

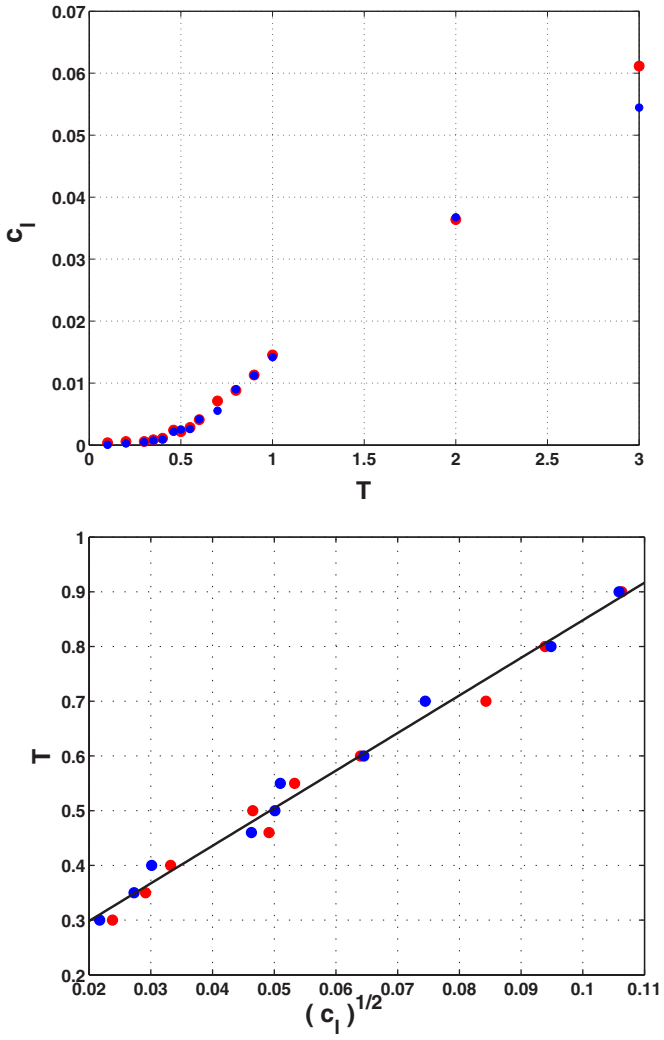

FIG. 2. (Color online). Concentration of defects under slow cooling. Upper panel: the concentration of the liquidlike defects: large particles in pentagons (red dots) and small particles in heptagons (blue dots). Lower panel: the fit of the concentration of liquidlike defects as a function of temperature according to Eq. (4).

(over all cells of the same type) of the potential energy $\epsilon_i = \left\langle \Sigma_{k=1}^{E_i} \epsilon \left(\frac{\sigma_{ik}}{r_{ik}}\right)^{12} \right\rangle$ where E_i is the number of edges associated with that cell type, and r_{ik} being the distance to the particle in the adjacent Voronoi cell. In Fig. 3, we present the values of these energies measured as a function of the temperature, following a protocol of slow cooling. There are ten different cell types in this system (large particle or small particle in squares, pentagons, hexagons, heptagons, and octagons), but octagons and squares are not shown since they disappear much before the glass transition. The lesson drawn from this graph is that the different cell types have clearly split energies throughout the interesting temperature range, and that these energies are only weakly dependent on the temperature. Within the temperature range of interest, we can focus on the six types of cells; denoted by $\{N_i\}_{i=1}^{6}$ the number of cells of each type, with number of edges E_i, ordering them by the energy ϵ_i from $i=1$ being the highest one (large particle in a pentagon) to $i=6$ being the small particle in a heptagon. Additional important properties of the cell types

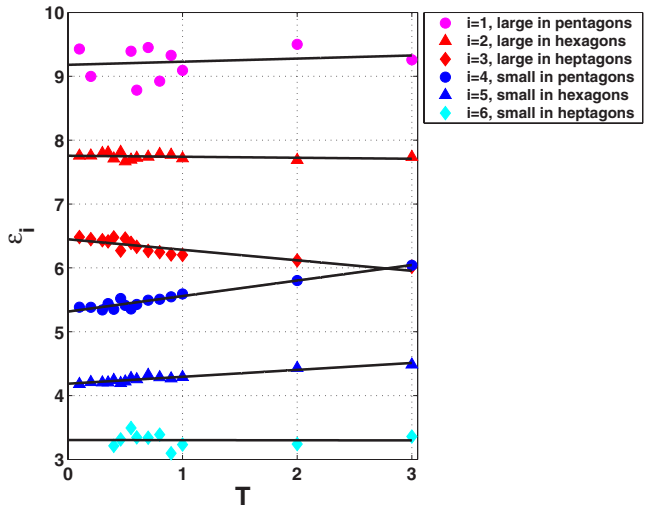

FIG. 3. (Color online). The average energies of the Voronoi cells as a function of the temperature as measured in the simulations.

are their areas Ω_i and their shapes; the first affects the enthalpy term and both affect the entropy when we count the number of possible tilings of the plane. With this in mind, we can construct the statistical mechanics of this system by considering the free energy $G=U+pV-TS$. The value of U is then simply $\Sigma_{i=1}^{6} N_i \epsilon_i$. The pV term is simply $p\Sigma_{i=1}^{6} N_i \Omega_i$. Lastly, we need to estimate the entropy term. In principle, this should be computed from the number of possible complete tilings of the area by N_i cells of each type with its given area and shape, subject to the Euler constraint $\Sigma_{i=1}^{6} N_i E_i = 6N$. This is a formidable problem. A useful estimate can be made by considering the area only, and filling space starting with the largest objects, then the next largest, etc. until the smallest is fit in. Denoting the possible number of boxes to fit the largest cells by $\mathcal{N}_1 \equiv V/\Omega_1$, then the number of boxes available for the second largest cell by $\mathcal{N}_2 \equiv (V-N_1\Omega_1)/\Omega_2$, etc., the number of possible configurations W is

$$W = \Pi_{k=1}^{6} \frac{\mathcal{N}_k!}{N_k!\,(\mathcal{N}_k - N_k)!}. \tag{6}$$

Denoting $x_i \equiv N_i/\mathcal{N}_i$, we compute directly $x_i = c_i\Omega_i/\Sigma_{j=i}^{6} c_j\Omega_j$, where c_i is the number concentration of each defect. We can now compute $S=k_B \ln W$ and write G together with a Lagrange multiplier for the Euler constraint,

$$G = \sum_{i=1}^{6} N_i\epsilon_i + p\sum_{i=1}^{6} N_i\Omega_i + \lambda\sum_{i=1}^{6} N_i E_i + T\sum_{k=1}^{6} \mathcal{N}_k[x_k \ln x_k + (1-x_k)\ln(1-x_k)]. \tag{7}$$

The chemical potential $\mu_i \equiv \partial G/\partial N_i$ is then

$$\mu_i = \epsilon_i + p\Omega_i + T\left(\ln x_i + \sum_{k=1}^{i-1} \frac{\Omega_i}{\Omega_k} \ln(1-x_k)\right) + \lambda E_i. \tag{8}$$

We now recognize that in equilibrium there exist only two independent values of μ_i, one for the small particles μ_S and one for the large particles μ_L, and we have nine unknowns—six values of c_i, 2 values of μ, and one Lagrange multiplier λ. This is precisely balanced by the six equations (8), the Euler constraint, and the two constraints $\Sigma_{i=1}^{3} c_i = \Sigma_{k=4}^{6} c_k = 1/2$. These equations can be solved numerically using the precise values of $\Omega_i(T)$ and $\epsilon_i(T)$ as measured in the simulation. The approximate calculation of the entropy, however, does not warrant such a detailed calculation. In reality, calculating the average areas of the cell types in the numerical simulations, we discover that to an excellent approximation these fall in two classes, smaller cells of area Ω_S when small particles are in them, and larger cells of area Ω_L when large particles are enclosed. These areas again are only weakly dependent on the temperature. Then the whole system of equations simplifies to two analytically tractable sets of equations

$$\tilde{\mu}_L = \epsilon_i + T \ln c_i + \lambda E_i \quad \{i = 1,2,3\},$$

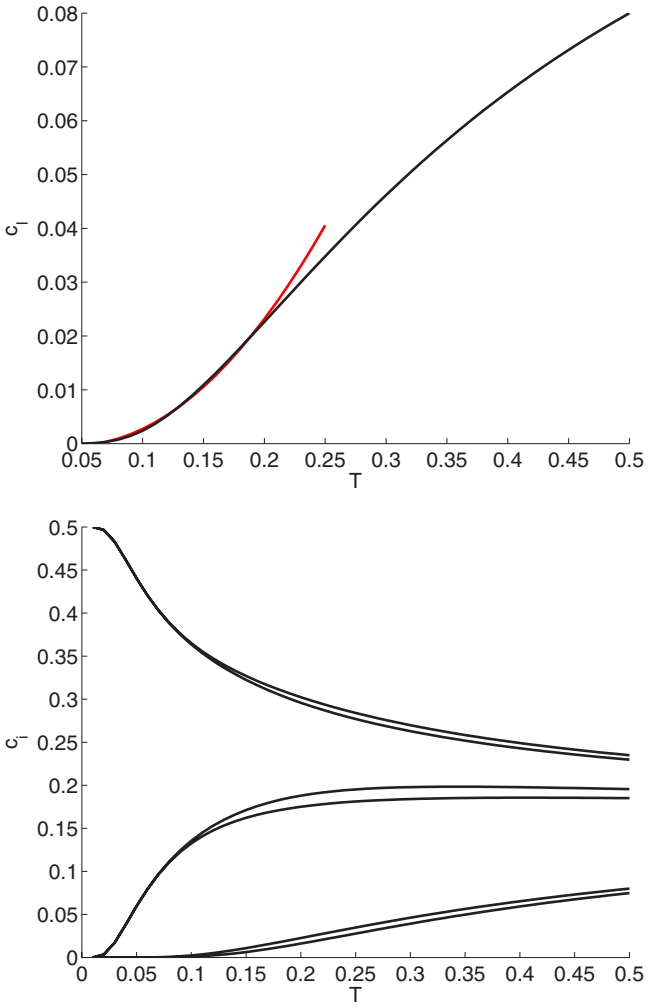

FIG. 4. (Color online). Upper panel: the concentration of the liquidlike defect (small in heptagon) as a function of temperature, together with the quadratic fit of the type Eq. (4). Lower panel: the concentrations of all the Voronoi cells as a function of T. Note the close-to-degeneracy of pairs of cells: the upper pair is the glasslike defects, the middle pair is the two hexagons, and the lower pair the liquidlike defects. Observe the existence of two temperatures, interpreted as T_g and T_c.

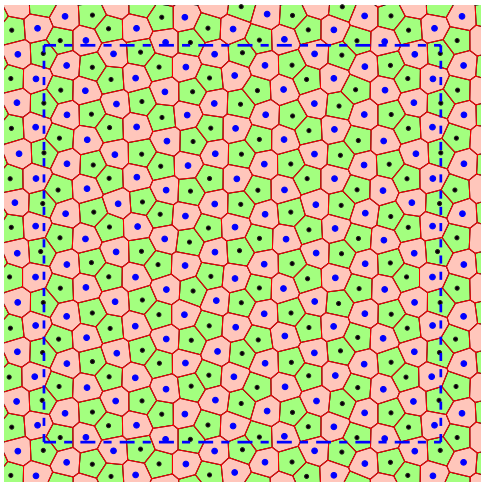

FIG. 5. (Color online). An example of a stable phase formed by glasslike defects at very low temperatures.

$$\tilde{\mu}_S = \epsilon_i + T \ln c_i + \lambda E_i \quad \{i = 4,5,6\}, \tag{9}$$

together with the above mentioned three constraints. In $\tilde{\mu}$, we have absorbed terms that added to μ in this special case.

In Fig. 4 we show the solutions of these equations when we use values of ϵ_i taken from the Fig. 3 at $T=0$ [9]. The results are in excellent agreement with the simulations. The curve associated with the temperature dependence of the concentration of the liquidlike defects can be very well fit by a quadratic fit like Eq. (4), with a temperature $T_g \approx 0.07$. In fact, the solution of Eqs. (9) shows that the concentrations do not quite vanish but become exponentially small, as stated above and in [6]. Note that the numerical value of T_g differs from the simulation, as is expected from a theory that does not take careful account of the correlations between different cells. The statistical mechanics predicts a second transition (see left panel of Fig. 4). There is a temperature T_c where the concentration of hexagonal cells is predicted to be exponentially small, and the system remains only with glasslike "defects." This prediction can be checked by simulations. Indeed, we found that phases made of only pentagons with small particles and heptagons with large particles exist and are stable at low temperatures, see Fig. 5. Upon warming such a phase up, at T_c, a sizable number of hexagons appears to form the generic glassy state. Upon further warming, at T_g, a sizable number of liquidlike defects brings the system to a liquid state. The actual values of T_g and T_c can be understood from this model. Denoted by c_ℓ, c_H, and c_G the concentrations of the liquidlike, hexagons, and glasslike defects, and by $\epsilon_\ell = \epsilon_1 + \epsilon_6 \approx 12.48$ the energy associated with the liquidlike defects, by $\epsilon_H = \epsilon_2 + \epsilon_5 \approx 11.94$ the energy of the hexagons, and $\epsilon_G = \epsilon_3 + \epsilon_4 \approx 11.76$ the energy of the glasslike defects. The theory predicts that ratios c_ℓ / c_H and c_H / c_G are of the order of $\exp[-(\epsilon_\ell - \epsilon_H)/T]$ and $\exp[-(\epsilon_H - \epsilon_G)/T]$, respectively. As an estimate of T_g and T_k take these ratios to be, say, of the order of $1\% \sim \exp(-5)$ and observe that such ratios are obtained for $T = T_g \approx 0.11$ and $T = T_c \approx 0.04$. It is important to notice that $\epsilon_H - \epsilon_G$ could be positive rather than negative, and then the system would crystallize on a hexagonal lattice. Such a lattice can exist in this system only when the particle's phase separates into two pure hexagonal lattices of small and large particles, respectively, with an interface in between. Such a phase may be even by the ground state, but seems to be inaccessible in dynamical experiments starting from random organizations of small and large particles. As the energies displayed in Fig. 3 were measured from the dynamics, our statistical mechanics does not reflect the possibility of phase separation.

CONCLUSIONS

It is quite remarkable that one can understand the properties of a system of strongly interacting particles in an essentially jammed state using the statistical mechanics of a mobile set of essentially noninteracting quasiparticles. Without any free parameter, we have offered a semiquantitative understanding of the features of the glass transition in this system, as well as the existence of two distinct temperatures T_g and T_c.

ACKNOWLEDGMENTS

This work was supported in part by the Israel Science Foundation, by the Minerva Foundation Munich, Germany, and by the German-Israeli Foundation.

[1] E. Donth, *The Glass Transition* (Springer, Berlin, 2001); P. G. Debenedetti and F. H. Stilliner, Nature (London) **410**, 259 (2001); K. Binder and W. Kob, *Glassy Materials and Disordered Solids* (World Scientific, Singapore, 2005); M. D. Ediger, Annu. Rev. Phys. Chem. **51**, 99 (2000).

[2] D. L. Price and J. M. Carpenter, J. Non-Cryst. Solids **92**, 153 (1987); J. Horbach and W. Kob, Phys. Rev. B **60**, 3169 (1999); L. Berthier, G. Biroli, J.-P. Bouchaud, L. Cipelletti, D. El Masri, D. L'hôte, F. Ladueu, and M. Pierno, Science **310**, 1797 (2005).

[3] D. N. Perera and P. Harrowell, Phys. Rev. E **59**, 5721 (1999), and references therein.

[4] J. P. Garrahan and D. Chandler, Proc. Natl. Acad. Sci. U.S.A. **100**, 9710 (2003); F. Ritort and P. Sollich, Adv. Phys. **52**, 219 (2003).

[5] D. Deng, A. S. Argon, and S. Yip, Philos. Trans. R. Soc. London, Ser. A **329**, 549 (1989); **329**, 575 (1989); **329**, 595 (1989); **329**, 613 (1989).

[6] E. Aharonov, E. Bouchbinder, V. Ilyin, N. Makedonska, I. Procaccia, and N. Schupper, Europhys. Lett. **77**, 56002 (2007).

[7] For similar ideas in arresting lattice models see, e.g., A. Lawlor, D. Reagan, G. D. McCullagh, P. De Gregorio, P. Tartaglia, and K. A. Dawson, Phys. Rev. Lett. **89**, 245503 (2002); A. Lawlor, P. De Gregorio, P. Bradley, M. Sellitoo, and K. A. Dawson, Phys. Rev. E **72**, 021401 (2005).

[8] D. Weaire and S. Hutzler, *Physics of Foams* (Clarendon Press, Oxford, 1999).

[9] Endowing the individual energies with the measured temperature dependence did not result in an important change in the statistical mechanics.